Am J Physiol Cell Physiol 330: C1800–C1811, 2026.
First published May 12, 2026; doi:10.1152/ajpcell.00159.2026

american physiological society

AMERICAN JOURNAL OF PHYSIOLOGY
CELL PHYSIOLOGY

RESEARCH ARTICLE

Dietary supplementation with ursolic acid preserves skeletal muscle mass and strength in mouse models of cancer cachexia

Jeremy B. Ducharme,[1]* Scott M. Ebert,[2,3,4]* Miles E. Cameron,[1,5] Martin M. Schonk,[1] Chandler S. Callaway,[1] Andrew C. D'Lugos,[1] John J. Talley,[4] Sarah M. Judge,[1,6,7] Christopher M. Adams,[2,3,4] and Andrew R. Judge[1,4,6,7]

[1]Department of Physical Therapy, University of Florida, Gainesville, Florida, United States; [2]Division of Endocrinology, Diabetes, Metabolism, and Nutrition, Department of Medicine, Mayo Clinic, Rochester, Minnesota, United States; [3]Department of Biochemistry and Molecular Biology, Mayo Clinic, Rochester, Minnesota, United States; [4]Emmyon, Inc., Rochester, Minnesota, United States; [5]Department of Surgery, University of Florida Health Science Center, Gainesville, Florida, United States; [6]Myology Institute, University of Florida, Gainesville, Florida, United States; and [7]Health Cancer Institute, University of Florida, Gainesville, Florida, United States

Abstract

Skeletal muscle atrophy is a devastating and defining feature of cancer cachexia that reduces quality of life, treatment tolerance, and survival, but cannot be prevented or reversed by current management strategies. Ursolic acid is a natural dietary compound that has been shown to inhibit atrophy-associated changes in skeletal muscle mRNA expression in rodents and dogs, leading to beneficial changes in skeletal muscle structure and function. We hypothesized that dietary supplementation with ursolic acid might help support skeletal muscle mass and function during cancer. To test this hypothesis, we investigated ursolic acid's effects in five in vivo mouse models of cancer cachexia that are driven by pancreatic, colon, and lung cancer cells of mouse and human origin. We found that dietary supplementation with ursolic acid has broad-spectrum effects toward cancer-induced skeletal muscle atrophy, significantly preserving muscle mass in all five cancer cachexia models. Ursolic acid's positive effects on muscle mass and muscle fiber size led to significant improvements in grip strength and muscle tetanic force, persisted in the presence of chemotherapy, and were not associated with discernible changes in food intake or tumor growth. Ursolic acid appeared to generate its beneficial effects in skeletal muscle by acting directly on muscle cells, inhibiting catabolic effects of tumor-derived secreted factors, and inhibiting >90% of cancer-induced changes in skeletal muscle mRNA expression. These results strongly nominate ursolic acid as a promising potential nutritional approach for supporting muscle mass and function in individuals with cancer.

NEW & NOTEWORTHY Cancer-induced muscle wasting affects many people with cancer, reducing treatment tolerance and survival. We identified a natural dietary compound, ursolic acid, that attenuates muscle atrophy across five preclinical cancer models spanning pancreatic, colon, and lung cancer. Ursolic acid inhibits cancer-induced changes in muscle mRNA expression, preserves muscle strength, and remains protective during chemotherapy, without affecting food intake or tumor burden. These results identify ursolic acid as a promising, translatable dietary supplement for supportive cancer care.

cancer cachexia; muscle atrophy; nutrition; skeletal muscle; ursolic acid

INTRODUCTION

Many types of cancer can induce severe generalized skeletal muscle atrophy and loss of body weight, also known as cancer cachexia. Cancer-induced muscle atrophy is especially prevalent in patients with pancreatic, colon, or lung cancer, where cachexia often presents as the first sign of cancer and has a major impact on cancer management and outcomes (1). Deleterious effects of cancer-induced muscle atrophy include weakness, fatigue, frailty, decreased quality of life, reduced fitness for tumor-directed therapies, and decreased survival (2, 3). However, despite its broad clinical impact, cancer-induced muscle atrophy cannot be reliably prevented or treated by current approaches, which include tumor-directed therapies, exercise, standard nutritional support, and appetite stimulants (4). Identifying new ways to better protect skeletal muscle mass and function could have important benefits for many patients.

The pathogenesis of cancer-induced muscle atrophy is complex and multifactorial in nature, with varying contributions

*J. B. Ducharme and S. M. Ebert contributed equally to this work.
Correspondence: C. M. Adams (adams.christopher2@mayo.edu); A. R. Judge (arjudge@phhp.ufl.edu).
Submitted 18 March 2026 / Revised 14 April 2026 / Accepted 4 May 2026

from tumor-derived factors, anorexia, malnutrition, muscle disuse, and tumor-directed therapies, often superimposed upon a background of advanced age and other illnesses and medications that promote muscle atrophy. This complexity can create challenges in designing therapies for cancer-induced muscle atrophy. However, all types of skeletal muscle atrophy, regardless of the underlying cause(s), involve and require numerous transcriptional changes within skeletal muscle fibers, including induction of mRNAs that promote muscle atrophy and weakness, and repression of mRNAs that are essential for maintenance of normal muscle mass and function (5). The set of mRNAs whose levels increase or decrease in skeletal muscle as it undergoes atrophy is called an mRNA expression signature of muscle atrophy and is mechanistically important because it captures the combined output of all of the upstream signaling pathways that generate the changes in mRNA expression, which in turn are essential for the pathogenesis of muscle atrophy and weakness (5, 6). Furthermore, mRNA expression signatures of muscle atrophy can be used to search for candidate inhibitors of skeletal muscle atrophy (5).

In previous work, we searched for small molecules whose mRNA expression signatures in human cell lines negatively correlate to mRNA expression signatures of skeletal muscle atrophy in humans and mice (6). Our screen discovered ursolic acid, a natural dietary compound found in several edible fruits and herbs, as a candidate small molecule inhibitor of muscle atrophy (6, 7). In subsequent studies, we and others found that ursolic acid acts directly on skeletal muscle, where it generates changes in mRNA expression by activating antiatrophy (anabolic) signaling through the insulin/IGF-1 pathway, and inhibiting proatrophy (catabolic) signaling through the forkhead box O (FOXO), activating transcription factor 4 (ATF4)-CCAAT/enhancer-binding protein β (C/EBPβ), myostatin, signal transducer and activator of transcription 3 (STAT3), and nuclear factor kappa B (NF-κB) signaling pathways (6, 8–11). As a result of its molecular effects in skeletal muscle, ursolic acid decreases muscle atrophy and weakness in mouse models of fasting, muscle disuse, advanced age, uremia, and spinal cord injury (6, 9, 10, 12). Moreover, in healthy mice lacking a stimulus for muscle atrophy, ursolic acid promotes muscle hypertrophy and increases strength and endurance exercise capacity (8, 9). Based on these findings and ursolic acid's favorable safety profile, ursolic acid is now becoming available as a dietary supplement and functional food ingredient for maintaining muscle health in companion animals and humans (13).

In the current study, we tested the hypothesis that dietary supplementation with ursolic acid might have beneficial effects toward cancer-induced skeletal muscle atrophy and weakness. To test this hypothesis, we used mouse models of cancer cachexia and investigated the effects of diet supplemented with ursolic acid.

METHODS

Animals

All animal procedures were approved by the University of Florida Institutional Animal Care and Use Committee (IACUC). C57Bl/6J mice (stock no: 000664) and NOD.Cg-Prkdc^{scid} Il2rg^{tm1Wjl}/SzJ (NSG) mice (stock no: 005557) were purchased from The Jackson Laboratory (Bar Harbor, ME). CD2F1 mice (stock no: 033) were purchased from Charles River Laboratories (Wilmington, MA). All mice were males, aged 10–12 wk. Mice were colony caged in a temperature-controlled facility with a 12-h light/dark cycle, with ad libitum access to food and water.

Mouse Diets

Ursolic acid was obtained from Enzo Life Sciences and incorporated into standard chow (NIH-31-modified open-formula mouse diet; Inotiv, Indianapolis, IN) at a concentration of 0.27% (wt/wt), as described previously (6, 8, 9). Control diet was standard chow lacking ursolic acid.

Cell Lines

Murine KPC pancreatic cancer cells (KPC FC1245 pancreatic cancer cells isolated from the tumor of an LSL-Kras$^{G12D/+}$; LSL-Trp53$^{R172H/+}$; Pdx-1-Cre mouse) (14) were generously provided by Dr. David Tuveson (Cold Spring Harbor Laboratory). Murine colon 26 adenocarcinoma (C26) cells and murine Lewis lung carcinoma (LLC) cells were obtained from the National Cancer Institute (NCI) Cell Repository (Bethesda, MD). Human PANC-1 pancreatic cancer cells, human HCT116 colon cancer cells, and murine C2C12 myoblasts were purchased from American Type Culture Collection (Rockville, MD). All cell lines were maintained at 37°C and 5% CO_2 in medium A.

Tissue Culture Media

Medium A is Dulbecco's Modified Eagle Medium (DMEM) containing 10% (vol/vol) fetal bovine serum and antibiotics (1% penicillin/streptomycin). Medium B is DMEM containing antibiotics and no serum. Medium C is DMEM containing 2% (vol/vol) horse serum and antibiotics. Medium D is 75% (vol/vol) medium C plus 25% (vol/vol) conditioned media (CM) from KPC pancreatic cancer cells. Conditioned media from KPC cells were collected and stored as previously described (15). In brief, KPC cells were plated in a T-25 cell culture flasks in medium A at 1×10^6 cells per flask for 24 h, rinsed twice with phosphate-buffered saline (PBS), rinsed three times with medium B, and then cultured for 24 h in medium B before collection of media, which was then centrifuged at 2,000 *g* for 15 min at 4°C, passed through a 0.22 μm filter, and stored at −80°C until use.

Mouse Models of Cancer Cachexia

We used five mouse models of cancer cachexia that utilized either mouse KPC pancreatic cancer cells, mouse C26 colon cancer cells, mouse LLC lung cancer cells, human HCT116 colon cancer cells, or human PANC-1 pancreatic cancer cells, as described previously (16–20). In the KPC model, pancreases of C57Bl/6J mice were surgically exposed and injected with 50 μL sterile saline containing 1.5×10^5 KPC cells. In the C26 model, bilateral flanks of CD2F1 mice were injected with 100 μL sterile saline containing 0.5×10^6 C26 cells. In the LLC model, bilateral flanks of C57Bl/6J mice were injected with 100 μL sterile saline containing 2.5×10^6 LLC cells. In the HCT116 model, bilateral flanks of NSG mice were injected with 100 μL sterile saline containing 3.0×10^6

HCT116 cells. In the PANC-1 model, pancreases of NSG mice were surgically exposed and injected with 50 µL sterile saline containing 0.5×10^6 PANC-1 cells. In all models, animals in the sham groups received injections of sterile saline lacking cells. In all models, mice were weighed between 0900 and 1000 h immediately before injections, every 3 days until tumors became palpable and then every day after tumors were palpable. In the KPC model, food intake was recorded daily between 0900 and 1000 h, beginning 3 days after pancreatic injections. To assess food intake, the chow present in the metal cage top, along with any spilled material collected from the bedding, was collected and weighed, and intake per cage was calculated as the difference between the prior day and the sum of the total chow remaining, then divided by the number of mice per cage. In some experiments, KPC tumor-bearing mice received intraperitoneal injections of 5-fluorouracil (25 mg/kg) beginning when tumors first became palpable and then every other day for 10 days, for a total of five injections, as described previously (21). In all models, mice were euthanized when tumor-bearing mice in the control diet group (standard chow without ursolic acid) reached the University of Florida IACUC mandated end point, based on body condition score and/or body mass loss.

Grip Strength and Muscle Contractility Assessments

Forelimb grip strength was determined using a BIO-GS4 grip strength meter (BIOSEB, North Pinellas Park, FL). Each mouse was subjected to three consecutive tests to obtain the peak value. In vitro muscle contractile function was assessed at the Physiological Assessment Core of the University of Florida, as previously described (22). In brief, freshly isolated extensor digitorum longus muscles were mounted on a force transducer (dual-mode lever system from Aurora Scientific, ON, Canada), which was then placed in a bath containing Ringer's solution at 22°C with 95% O_2 and 5% CO_2. After determining the optimal muscle length, maximum isometric twitch and tetanic forces were measured using a single supramaximal stimulation and a 500-ms train at 150 Hz, respectively, with a 5-min rest period between each set. Muscles were then stimulated at frequencies ranging from 5 to 150 Hz to establish the force-frequency relationship. Specific force was calculated by normalizing maximal tetanic force to muscle cross-sectional area (CSA), as described previously (23).

Histological Analyses of Skeletal Muscle

Mouse skeletal muscles (tibialis anterior and diaphragm) were dissected and immediately placed in optimal cutting temperature compound (Tissue-Tek), then frozen in liquid isopentane cooled with liquid nitrogen and stored at −80°C until cryosectioning. Cryosectioning was performed by incubating the embedded muscles at −20°C for 1 h and then using a microtome cryostat to obtain serial 10-µm-thick skeletal muscle sections, which were then transferred to positively charged glass slides. Cryosections were then rinsed three times with PBS, incubated in PBS containing 10% normal goat serum and a 1:300 dilution of Alexa Fluor 594-conjugated wheat germ agglutinin (W11262; Invitrogen) for 1 h at 22°C. Sections were then rinsed three times with PBS, mounted in ProLong Diamond Antifade Mountant (Invitrogen), and overlayed with a coverslip. Immunofluorescence microscopy and image acquisition were performed with a Leica DM5000B microscope (Leica Microsystems) equipped with a DFC340 FX digital camera, a Leica N2.1filter cube, and a Leica Application Suite (LAS) software package, using a ×10 objective for imaging of tibialis anterior myofibers and a ×20 objective for imaging of diaphragm myofibers. Image analysis and determination of myofiber cross-sectional area (CSA) was performed with Cellpose and the "LabelsToROIs" ImageJ plug-in, and ImageJ region of interest (ROI) color coder was used to color myofibers on a gradient according to their CSA, as previously described (24).

RNA Sequencing

Mouse tibialis anterior skeletal muscles were dissected and immediately placed in liquid nitrogen and stored at −80°C, then shipped as frozen samples on dry ice to Azenta Life Sciences (South Plainfield, NJ) for RNA extraction, library preparation, and RNA sequencing (RNA-Seq). Total RNA was extracted using Qiagen RNeasy Plus Universal mini kit (Qiagen, Hilden, Germany). RNA samples were quantified using Qubit 2.0 Fluorometer (Life Technologies, Carlsbad, CA), and RNA integrity was checked using Agilent TapeStation 4200 (Agilent Technologies, Palo Alto, CA). RNA-Seq libraries were prepared from mRNA enriched using Oligo(dT) beads with the NEBNext Ultra RNA Library Prep Kit for Illumina (NEB, Ipswich, MA). Enriched mRNA was fragmented (15 min, 94°C), and first- and second-strand cDNA synthesis was performed. cDNA fragments were end-repaired, adenylated at the 3′ ends, ligated to universal adapters, indexed, and PCR-enriched. Libraries were validated on the Agilent TapeStation 4200 and quantified using a Qubit 2.0 Fluorometer and quantitative PCR (KAPA Biosystems, Wilmington, MA). Sequencing libraries were clustered on two flowcell lanes and sequenced on an Illumina HiSeq 2000 using a 2×150 bp paired-end configuration. Image analysis and base calling were performed with Illumina Control Software, and raw .bcl files were converted to FASTQ and demultiplexed using bcl2fastq (v2.17). Reads were trimmed to remove adapters and low-quality bases, then aligned to the *Mus musculus* GRCm38 ENSEMBL genome using STAR (v2.5.2b). Unique gene counts were obtained with FeatureCounts from the Subread package (v1.5.2), considering only reads uniquely mapped to exons. Differential expression analysis was performed with DESeq2 using Wald tests, with P values adjusted by the Benjamini–Hochberg method to control the false discovery rate (FDR q-values).

Intraperitoneal Injections of Ursolic Acid

In Supplemental Fig. S2, mice received twice-daily intraperitoneal injections of ursolic acid (200 mg/kg in corn oil) or volume-matched vehicle (corn oil), as previously described (6).

In Vitro Model of Cancer-Induced Muscle Atrophy

C2C12 myoblasts were cultured in medium C for 5 days to generate fully differentiated C2C12 myotubes, which were then incubated for 48 h in either medium C (lacking tumor-conditioned media) or medium D (25% tumor-conditioned media) containing either vehicle (0.1% DMSO) or 1 µM

ursolic acid. Myotubes were then rinsed with PBS, fixed in PBS containing 2% paraformaldehyde (Boston BioProducts, Ashland, MA) for 30 min at 22°C, rinsed with PBS, permeabilized and blocked in PBS containing 3% bovine serum albumin (BSA) and 0.5% Triton X-100 for 30 min at 22°C, incubated in PBS containing 3% BSA and a 1:200 dilution of mouse monoclonal antimyosin heavy chain antibody MF20 (Developmental Studies Hybridoma Bank, Iowa City, IA) overnight at 4°C, rinsed three times with PBS, incubated in PBS containing 3% BSA and a 1:500 dilution of goat anti-mouse IgG conjugated to Rhodamine Red-X (Thermo Fisher Scientific) for 1 h at 22°C, and then rinsed again with PBS. Immunofluorescence microscopy and image acquisition were performed with a ×20 objective on a Leica DMI3000B inverted microscope (Leica Microsystems) equipped with a DFC340 FX digital camera, Leica A4 and N2.1 filter cubes, and the LAS software package. Image analysis was performed using ImageJ software. Myotube diameter was determined by averaging at least two width measurements per myotube from at least 150 myotubes per group.

Statistical Analysis

When applicable, individual data points are shown, and group data are presented as means ± standard error. Before all parametric analyses, data distributions were assessed for normality using the Shapiro–Wilk test. Comparisons between two groups were made using Student's two-tailed *t* test. For comparisons involving more than two groups, ANOVAs with Tukey's post hoc analyses were performed. RStudio (v2024.12.1) and GraphPad Prism (v10.2.3) were used for data analysis, and statistical significance was set to $P < 0.05$ unless otherwise stated.

RESULTS

Dietary Supplementation with Ursolic Acid Reduces Skeletal Muscle Atrophy and Weakness in a Mouse Model of Pancreatic Cancer

As an initial test of ursolic acid's potential efficacy against cancer-induced muscle atrophy, we used a well-established model of pancreatic ductal adenocarcinoma (17, 25, 26). In this model, cultured pancreatic adenocarcinoma cells that express constitutively active Kras and dominant-negative p53 (KPC cells) are orthotopically transplanted into the pancreases of tumor-free mice, leading to the development of pancreatic tumors, followed by cancer-induced muscle atrophy and weakness.

To determine the effect of ursolic acid, we supplemented standard mouse chow with 0.27% ursolic acid, which has been shown to decrease muscle atrophy and weakness in cancer-free mice (6, 9). We then provided mice with KPC pancreatic tumors ad libitum access to standard chow lacking or containing ursolic acid. As expected, in the absence of ursolic acid, KPC tumors induced profound weight loss (Fig. 1*A*) and anorexia (Fig. 1*B*). However, dietary supplementation with ursolic acid significantly inhibited cancer-induced weight loss (Fig. 1*A*) without increasing food intake (Fig. 1*B*) or inhibiting tumor growth (Fig. 1*C*).

Importantly, ursolic acid-mediated preservation of body weight was explained by a reduction in cancer-induced

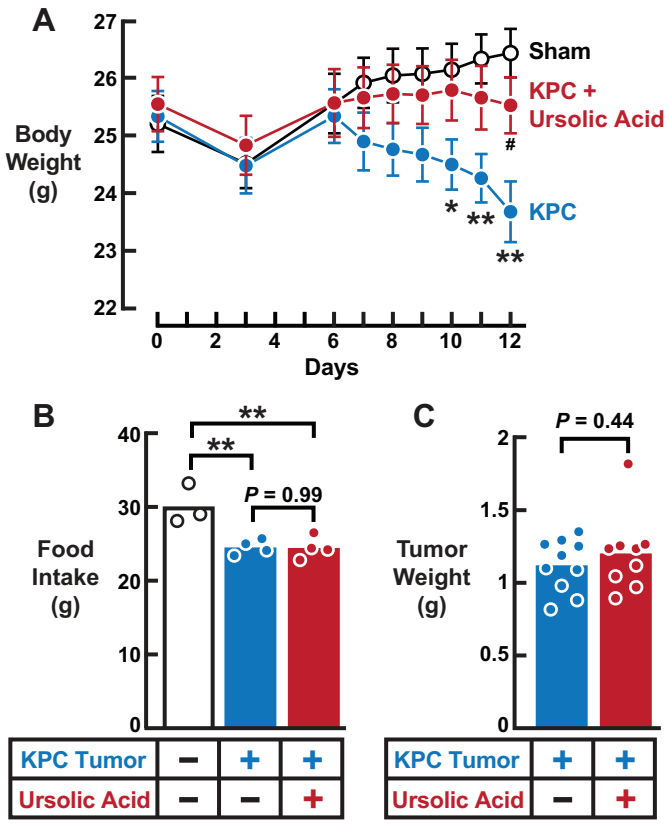

Figure 1. Ursolic acid reduces cachexia in a mouse model of pancreatic cancer. Eleven-week-old male C57BL/6 mice were administered intrapancreatic injections of either saline ("Sham") or KPC pancreatic cancer cells ("KPC"). On *day 5*, when KPC mice began to exhibit palpable tumors, a portion of KPC mice were randomly selected to receive ad libitum access to standard chow containing 0.27% ursolic acid ("KPC + Ursolic Acid"). The remaining mice ("Sham" and "KPC") continued to receive ad libitum access to standard chow lacking ursolic acid. Body weight and food intake were monitored. On *day 12*, KPC mice (± ursolic acid) were euthanized for assessment of tumor weight. *A*: body weight. Data are presented as means ± SE from 7 to 10 mice per group. *P* values were determined by two-way ANOVA with Tukey's posttest. $*P < 0.05$; $**P < 0.01$ in sham vs. KPC; $\#P < 0.05$ in KPC vs. KPC + Ursolic Acid. *B*: cumulative food intake during the treatment period (*days 5–12*). Each symbol represents the average from one cage (1–3 mice per cage), horizontal bars denote means, and *P* values were determined with one-way ANOVA with Tukey's posttest. $**P < 0.01$. *C*: tumor weight. Each symbol represents data from one mouse, and horizontal bars denote means. *P* value was determined with an unpaired two-tailed *t* test.

skeletal muscle atrophy. In the absence of ursolic acid, KPC pancreatic tumors induced skeletal muscle atrophy and weakness, as indicated by reductions in muscle mass (Fig. 2, *A–C* and *F*), decreased grip strength (Fig. 2, *D* and *E*), reduced tetanic force (Fig. 2, *G* and *H*), and decreased skeletal myofiber size (Fig. 3, *A–F*). Dietary supplementation with ursolic acid significantly inhibited all of these effects of KPC pancreatic tumors, leading to preservation of skeletal muscle mass (Fig. 2, *A–C* and *F*), grip strength (Fig. 2, *D* and *E*), tetanic force (Fig. 2, *G* and *H*), and skeletal myofiber size (Fig. 3, *A–F*). Specific force was not altered by KPC pancreatic tumors or ursolic acid under these conditions (Fig. 2*I*).

Interestingly, dietary supplementation with ursolic acid had similar effects if it was initiated after tumors had reached a palpable size (as in Figs. 1, 2, and 3) or before cancer had

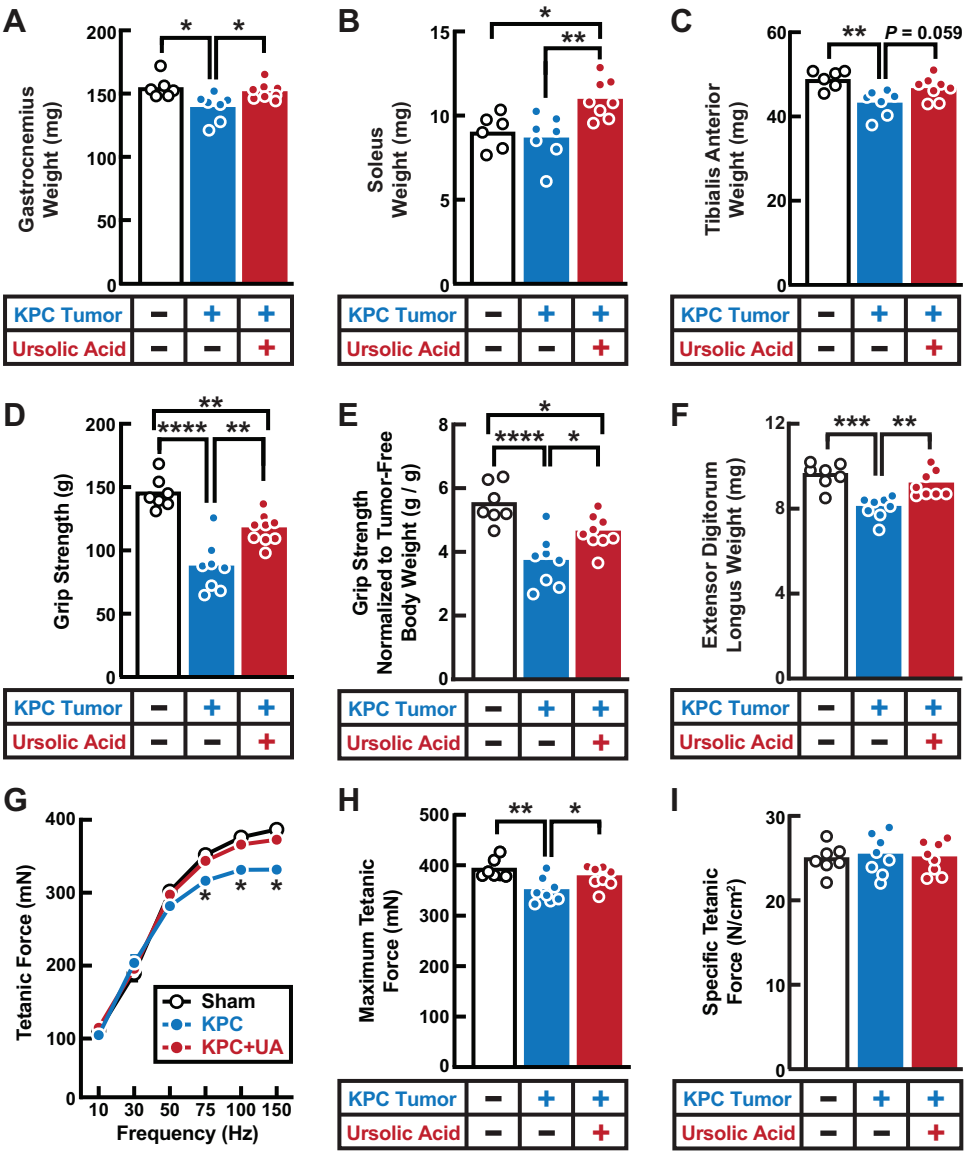

Figure 2. Ursolic acid reduces muscle wasting and weakness in a mouse model of pancreatic cancer. Eleven-week-old male C57BL/6 mice were administered intrapancreatic injections of either saline ("Sham") or KPC pancreatic cancer cells ("KPC"). On *day 5*, a portion of KPC mice were randomly selected to receive ad libitum access to standard chow containing 0.27% ursolic acid ("KPC + Ursolic Acid"). The remaining mice ("Sham" and "KPC") continued to receive ad libitum access to standard chow lacking ursolic acid. On *day 12*, grip strength was assessed, and then mice were euthanized for assessment of skeletal muscle mass and muscle contractile force. *A–C*: wet weights of gastrocnemius (*A*), soleus (*B*), and tibialis anterior (*C*) muscles; *D*: grip strength; *E*: grip strength normalized to tumor-free body weight; *F*: wet weight of extensor digitorum longus muscle; *G–I*: force frequency curves (*G*), maximal tetanic force (*H*), and specific force (*I*) from extensor digitorum longus muscles. In *A–F* and *H* and *I*, each symbol represents data from one mouse, horizontal bars denote means, and *P* values were determined by one-way ANOVA with Tukey's posttest. In *G*, data are presented as means ± SE from 7 to 8 mice per group, and *P* values were determined by two-way ANOVA with Tukey's posttest. $^{*}P < 0.05$; $^{**}P < 0.01$; $^{****}P < 0.0001$.

begun (Supplemental Fig. S1). In addition, we observed similar effects if ursolic acid was administered parenterally (Supplemental Fig. S2) rather than orally, or if dietary supplementation with ursolic acid was provided to tumor-bearing mice along with 5-fluorouracil chemotherapy (Fig. 4 and Supplemental Fig. S3). Collectively, these data indicated that ursolic acid has a capacity to decrease weight loss, muscle atrophy, and weakness in the mouse KPC model, without discernable effects on food intake or tumor growth.

Dietary Supplementation with Ursolic Acid Inhibits Cancer-Induced Changes in Skeletal Muscle mRNA Expression

In cancer-free animals, ursolic acid reduces muscle atrophy and weakness by inhibiting stress-induced changes in skeletal muscle mRNA expression (6, 9). To test the hypothesis that ursolic acid might have similar effects in the skeletal muscle of mice with pancreatic cancer, we isolated tibialis anterior muscles from KPC tumor-bearing animals that had received either standard chow or standard chow supplemented with ursolic acid. As a negative control, we isolated tibialis anterior muscles from tumor-free animals that had received standard chow lacking ursolic acid. We then performed comprehensive transcriptomic analyses (RNA-Seq) on the muscles from the three groups of mice (cancer-free control animals, cachectic KPC tumor-bearing animals with cancer-induced muscle atrophy, and KPC tumor-bearing animals who received dietary supplementation with ursolic acid).

As expected, in the absence of ursolic acid, pancreatic cancer induced widespread transcriptional changes in skeletal muscle, significantly altering levels of 18.9% of total mRNAs assessed (Fig. 5*A*). Many of the mRNAs that were induced by pancreatic cancer are known to promote muscle atrophy and weakness, including mRNAs that encode proatrophy transcription regulators (*Foxo1*, *Foxo3*, *Atf4*, *Cebpb*, *Cebpd*, *Klf10*, *Klf15*), proatrophy secreted factors (*Mstn*, *Inhbb*), proatrophy cell surface receptors (*Acvr1b*, *Tgfbr3l*, *Tgfbr3*, *Il6ra*), mediators of the ubiquitin-proteasome pathway (*Trim63*, *Fbxo32*, *Fbxo30*, *Fbxo31*, *Ubr2*, *Ubr4*, *Ube2o*, *Ube4a*, *Ube4b*, *Zfand5*, *Ubb*, *Ubc*, *Psma2*, *Psma5*, *Psma7*, *Psmb2*, *Psmb3*, *Psmd11*,

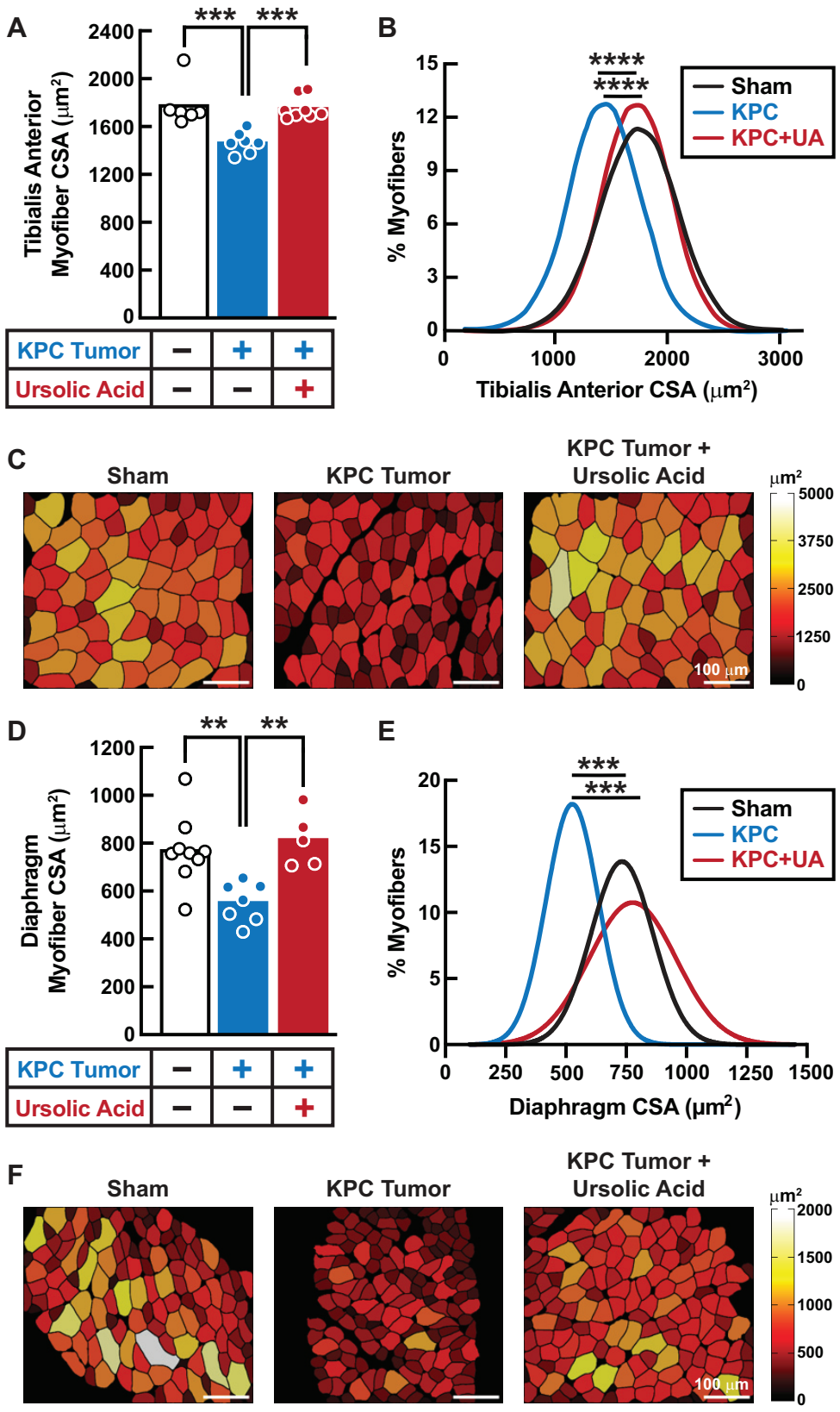

Figure 3. Ursolic acid inhibits cancer-induced skeletal myofiber atrophy. Eleven-week-old male C57BL/6 mice were administered intrapancreatic injections of either saline ("Sham") or KPC pancreatic cancer cells ("KPC"). On *day 5*, a portion of KPC mice were randomly selected to receive ad libitum access to standard chow containing 0.27% ursolic acid ["KPC + Ursolic Acid (UA)"]. The remaining mice ("Sham" and "KPC") continued to receive ad libitum access to standard chow lacking ursolic acid. On *day 12*, mice were euthanized for assessment of myofiber size in the tibialis anterior and diaphragm muscles. *A–C*: tibialis anterior mean cross-sectional area (CSA) (*A*), fiber size distribution curves (*B*), and representative cross-sections (*C*). *D–F*: diaphragm mean CSA (*D*), fiber size distribution curves (*E*), and representative cross-sections (*F*). In *A* and *D*, each symbol represents data from one mouse with 5 to 9 mice per group, horizontal bars denote means, and *P* values were determined by one-way ANOVA with Tukey's posttest. In *B* and *E*, data were binned and modeled with Gaussian least squares regression, and *P* values were determined by the extra sum-of-squares *F* test. $^{**}P < 0.01$; $^{***}P < 0.001$; $^{****}P < 0.0001$.

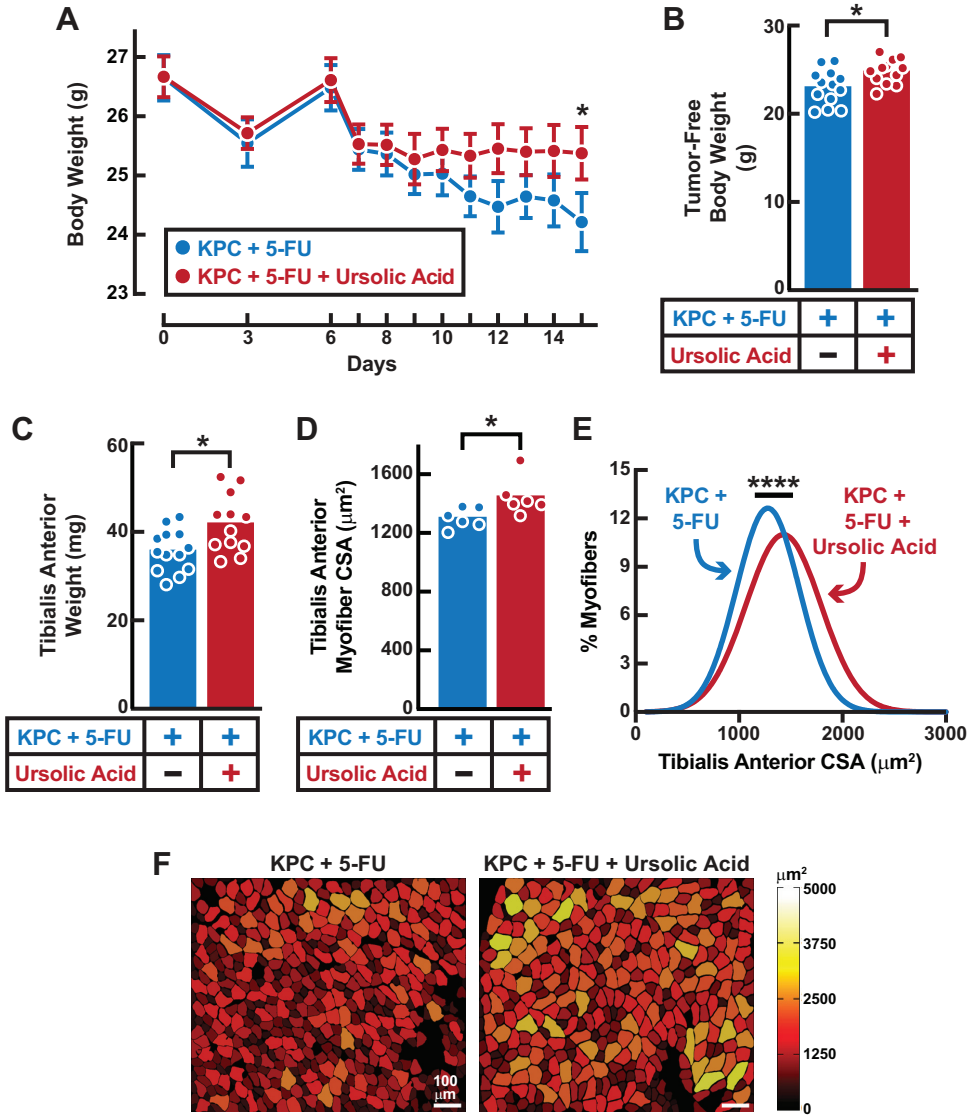

Figure 4. Ursolic acid reduces cachexia and muscle wasting in mice receiving chemotherapy for pancreatic cancer. Eleven-week-old male C57BL/6 mice were administered intrapancreatic injections of KPC pancreatic cancer cells. On *day 6*, mice began a 10-day course of 5-fluorouracil (5-FU) and were randomly divided into two groups, which received ad libitum access to either standard chow ("KPC + 5-FU") or standard chow containing 0.27% ursolic acid ("KPC + 5-FU + Ursolic Acid"). Body weight was monitored (*A*), and on *day 16*, mice were euthanized for assessment of tumor-free body weight (*B*), wet weights of tibialis anterior (TA) muscles (*C*), and TA mean cross-sectional area (CSA) (*D*), TA fiber size distribution curves (*E*), and representative TA cross-sections (*F*). In *A*, data are presented as means ± SE from 12 to 13 mice per group, and *P* values were determined by two-way ANOVA with Tukey's posttest. In *B*–*D*, each symbol represents data from one mouse, horizontal bars denote means, and *P* values were determined with unpaired two-tailed *t* tests. In *E*, data were binned and modeled with Gaussian least squares regression, and *P* values were determined by the extra sum-of-squares *F* test. $*P < 0.05$; $****P < 0.0001$.

Psmd2, *Psmd3*, *Psmd4*), mediators of autophagy (*Retreg1*, *Bnip3*, *Gabarapl1*, *Sqstm1*, *Map1lc3b*, *Ulk1*, *Atg13*, *Wipi2*, *Nbr1*, *Ctsl*), other atrophy mediators (*Gadd45a*, *Eif4ebp1*, *Ddit4*, *Mt1*, *Mt2*), and other atrophy markers (*Hmox1*, *Ern1*, *Sesn1*, *Serpine1*, *Fkbp5*, *Glul*, *Ampd3*, *Pdk4*) (Fig. 5*D* and Supplemental Table S1). Conversely, many of the mRNAs that were repressed by pancreatic cancer are known to be essential for maintenance of normal muscle mass and function, including mRNAs that encode antiatrophy transcription regulators (*Foxo6*, *Myod1*, *Perm1*, *Ppargc1b*), antiatrophy cell surface receptors (*Tas1r1*, *Aplnr*), antiatrophy myokines (*Apln*, *Igf1*, *Fstl1*, *Ostn*, *Metrnl*, *C1qtnf1*, *C1qtnf2*, *C1qtnf6*, *Adipoq*, *Ccdc80*, *Lum*, *Kera*), antiatrophy structural proteins (*Myoc*, *Fbn1*, *Myom3*), and proteins with key roles in calcium handling (*Casq1*), iron uptake (*Tfrc*), creatine synthesis (*Gatm*), glycolysis (*Pgam2*), glycophagy (*Stbd1*), lipolysis inhibition (*G0s2*), NAD+ synthesis (*Nmrk2*), protein quality control (*Mettl21c*), and polyamine metabolism (*Amd1*, *Amd2*, *Smox*) (Fig. 5*E* and Supplemental Table S1). These cancer-induced transcriptional changes in skeletal muscle were expected and are central to the pathogenesis of cancer-induced muscle atrophy and weakness.

Importantly, dietary supplementation with ursolic acid tended to normalize skeletal muscle mRNA expression in the presence of KPC pancreatic cancer. For example, in the presence of ursolic acid, pancreatic cancer significantly altered levels of only 1.3% of total mRNAs (Fig. 5*B*). Furthermore, skeletal muscle mRNAs that were increased by pancreatic cancer were decreased by ursolic acid and vice versa, indicating a highly significant negative correlation between the effects of cancer and the effects of ursolic acid (Fig. 5*C*). Specific effects of ursolic acid included repression/deinduction of mRNAs that promote muscle atrophy and weakness (Fig. 5*D*) and induction/derepression of mRNAs that are important for maintaining normal muscle mass and function (Fig. 5*E*). Thus, ursolic acid broadly inhibited cancer-induced changes in skeletal muscle mRNA expression, providing a likely explanation for how ursolic acid inhibits muscle atrophy and weakness in the KPC model of cancer cachexia.

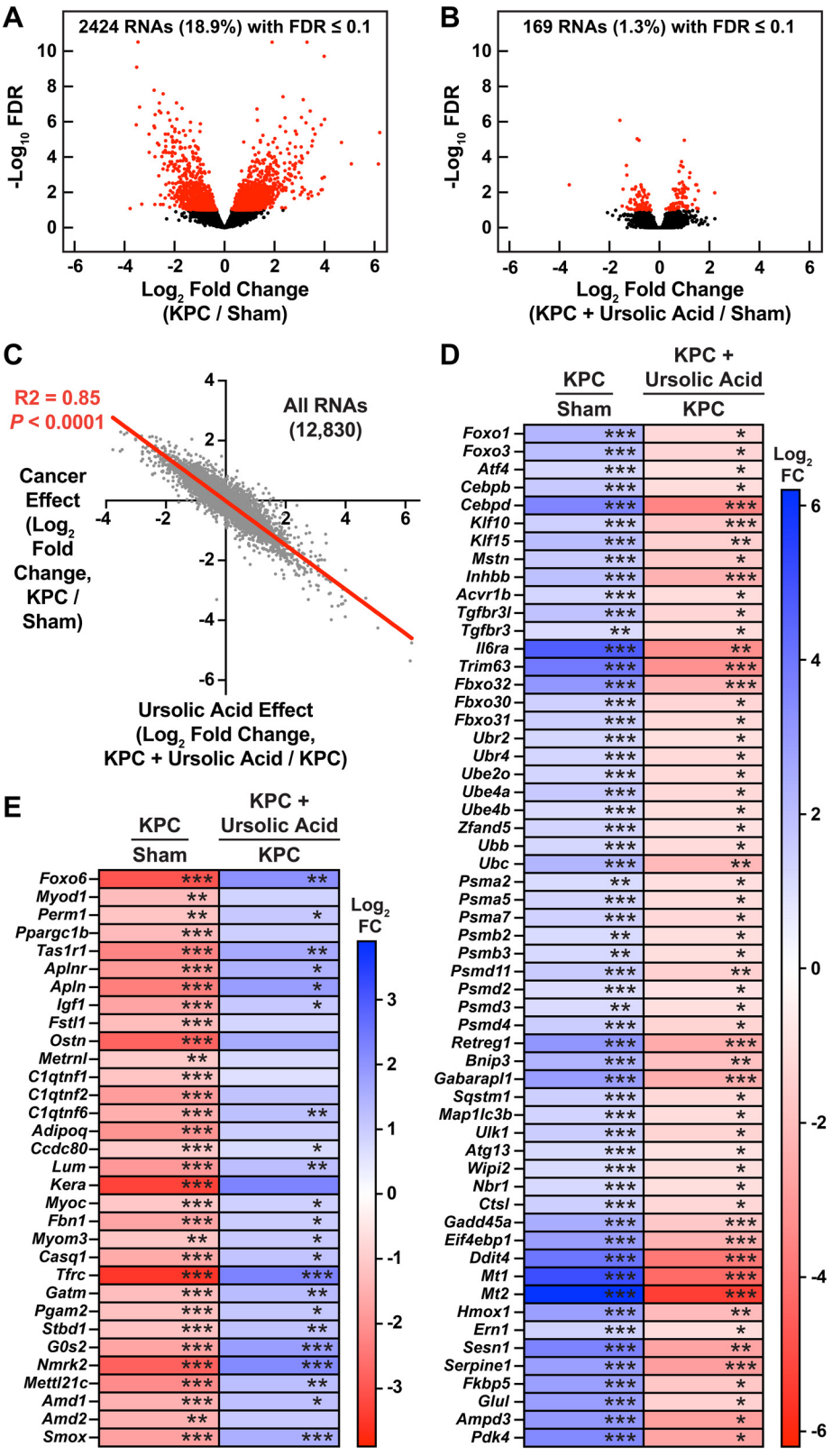

Figure 5. Ursolic acid inhibits cancer-induced changes in skeletal muscle mRNA expression. Eleven-week-old male C57BL/6 mice were administered intrapancreatic injections of saline ("Sham") or KPC pancreatic cancer cells ("KPC"). On *day 5*, a portion of KPC-injected mice were randomly selected to receive ad libitum access to standard chow containing 0.27% ursolic acid ("KPC + Ursolic Acid"), whereas the remaining mice ("Sham" and "KPC") continued to receive ad libitum access to standard chow lacking ursolic acid. On *day 12*, tibialis anterior muscles were collected for RNA-Seq analysis. Data are from four muscles per condition. *A* and *B*: volcano plots showing cancer-induced changes in skeletal muscle RNA expression in the absence (*A*) and presence (*B*) of ursolic acid. *C*: X-Y plot showing effect of pancreatic cancer (*x*-axis, KPC/Sham) vs. effect of ursolic acid (*y*-axis, KPC + ursolic acid/KPC) on levels of all 12,830 quantitated skeletal muscle RNAs. *D* and *E*: heat maps showing effect of pancreatic cancer (KPC/Sham) and effect of ursolic acid (KPC + ursolic acid/KPC) on representative mRNAs that promote muscle atrophy and weakness (*D*) and representative mRNAs that promote maintenance of normal muscle mass and function (*E*). *FDR $\leq$ 0.25; **FDR $\leq$ 0.10; ***FDR $\leq$ 0.05. FDR, false discovery rate.

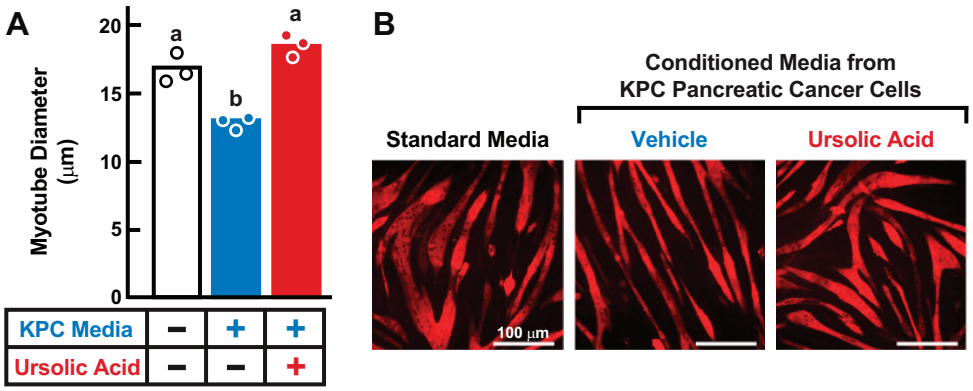

Figure 6. Ursolic acid inhibits effects of tumor-derived factors in an in vitro model of cancer-induced muscle atrophy. *A* and *B*: C2C12 myoblasts were cultured and fully differentiated into myotubes, then incubated for 48 h with either standard media or conditioned media obtained from cultures of KPC pancreatic cells (KPC-conditioned media), in the presence of either vehicle (DMSO) or 1 mM ursolic acid. Myotubes were then fixed and stained with myosin heavy chain antibody MF20 and subjected to fluorescence microscopy and image analysis. *A*: quantification of myotube diameter. Each symbol represents data from one experiment. Data are presented as means ± SE from ≥150 myotubes per group. Different letters denote statistically significant differences ($P \leq 0.05$) by one-way ANOVA with Tukey's posttest. *B*: representative images of myotubes.

Ursolic Acid Inhibits Effects of Tumor-Derived Factors in an In Vitro Model of Cancer-Induced Muscle Atrophy

Malignant tumors can secrete complex mixtures of catabolic factors that promote muscle atrophy (1). This process can be modeled in vitro by applying conditioned media from malignant cells to cultured skeletal myotubes, a cell culture model of skeletal muscle (27, 28). To test the hypothesis that ursolic acid might inhibit the effects of tumor-derived factors, we collected conditioned media (CM) from cultures of KPC pancreatic cells (KPC CM) and then applied it to cultures of skeletal myotubes in the absence and presence of ursolic acid. In the absence of ursolic acid, KPC CM induced myotube atrophy within 48 h, as expected (Fig. 6, *A* and *B*). However, ursolic acid inhibited the effect of KPC CM, preventing myotube atrophy (Fig. 6, *A* and *B*). These results suggest that ursolic acid inhibits KPC tumor-induced muscle atrophy, at least in part, by interfering with the actions of secreted tumor-derived catabolic factors.

Dietary Supplementation with Ursolic Acid Reduces Muscle Wasting in Four Additional Mouse Models of Cancer Cachexia Involving Tumors of Both Mouse and Human Origin

To test the hypothesis that ursolic acid might have broad-spectrum effects toward cancer-induced muscle atrophy, we investigated four additional mouse models of cancer cachexia. Two of these models employed mouse-derived tumor cells in immunocompetent mice (LLC and C26 models; Fig. 7), and two of these models employed human-derived tumor cells in immunocompromised mice (HCT116 and PANC-1 models; Fig. 8). Tumor cells were derived from lung cancer (LLC model), colon cancer (C26 and HCT116 models), and pancreatic cancer (PANC-1 model).

Similar to its effects in the KPC pancreatic cancer model, dietary supplementation with ursolic acid blunted cancer-induced muscle wasting in the LLC lung cancer model (Fig. 7, *A–C*), the C26 colon and HCT116 colon cancer models (Fig. 7, *D–F* and Fig. 8, *A–C*), and the PANC-1 pancreatic cancer model (Fig. 8, *D–F*), without affecting tumor size (Supplemental Fig. S4). These data indicate that ursolic acid has protective effects in at least five distinct mouse models of cancer-induced skeletal muscle atrophy, as well as a capacity to protect skeletal muscle from catabolic effects of human cancer cells.

DISCUSSION

In the current study, we aimed to identify a new nutritional approach that could help maintain muscle mass in individuals with cancer. To that end, we investigated the effects of a natural dietary compound, ursolic acid, in five distinct and complementary in vivo mouse models of cancer cachexia. We found that ursolic acid has broad-spectrum effects against cancer-induced muscle atrophy, protecting muscle mass from catabolic effects of pancreatic, colon, and lung cancer. In addition, ursolic acid's protective effects are observed in rapidly developing forms of cancer cachexia (as in the 12-day KPC model) and also in more slowly developing forms of cancer cachexia (as in the 48-day PANC-1 model). Moreover, the protection against muscle atrophy occurred without any discernible effects on tumor growth or food intake, occurred in the presence of both mouse and human cancer cells, and persisted in the presence of chemotherapy. Consistent with these findings, two other groups recently and independently reported that ursolic acid decreases cancer-induced muscle atrophy without impacting tumor growth in the mouse C26 and LLC models (11, 29). Collectively, these results strongly nominate ursolic acid as a promising potential nutritional approach for supporting muscle mass and function in individuals with cancer.

We also observed that dietary supplementation with ursolic acid has a remarkable capacity to inhibit cancer-induced changes in skeletal muscle mRNA expression. We believe this is a central mechanism by which ursolic acid helps to preserve muscle mass and strength. Ursolic acid's transcriptional effects are predicted to beneficially impact numerous cellular processes that control muscle mass and strength (including ubiquitin-proteasome, autophagy-lysosomal, inflammatory, metabolic, structural, and

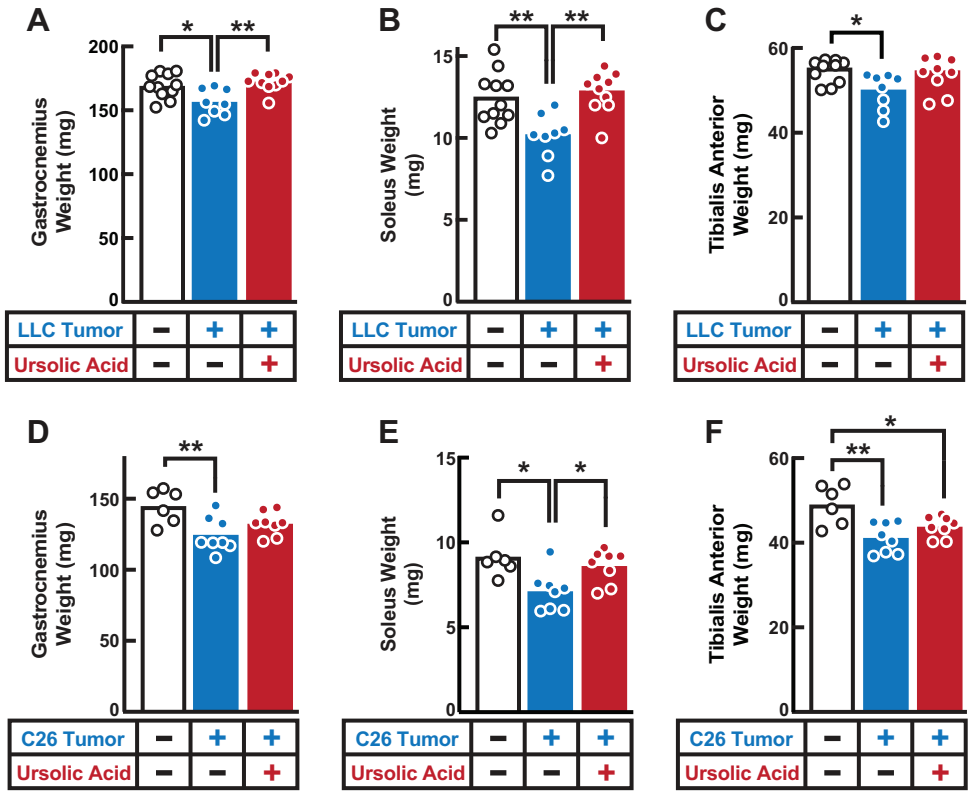

Figure 7. Ursolic acid reduces muscle wasting in mouse models of lung and colon cancer cachexia. *A–C*: ten-week-old male C57BL/6 mice were administered bilateral flank injections of either saline ("Sham") or Lewis lung carcinoma cells ("LLC"). On *day 6*, when LLC mice began to exhibit palpable tumors, half of LLC mice were provided ad libitum access to standard chow containing 0.27% ursolic acid ("LLC + Ursolic Acid"), and the remaining mice ("Sham" and "LLC") continued to receive ad libitum access to standard chow lacking ursolic acid. On *day 15*, mice were euthanized for assessment of gastrocnemius (*A*), soleus (*B*), and tibialis anterior (*C*) weights. *D–F*: ten-week-old male CD2F1 mice were administered bilateral flank injections of either saline ("Sham") or C26 colon adenocarcinoma cells ("C26"). On *day 8*, when C26 mice began to exhibit palpable tumors, half of C26 mice were provided ad libitum access to standard chow containing 0.27% ursolic acid ("C26 + Ursolic Acid"), and the remaining mice ("Sham" and "C26") continued to receive ad libitum access to standard chow lacking ursolic acid. On *day 22*, mice were euthanized for assessment of gastrocnemius (*D*), soleus (*E*), and tibialis anterior (*F*) weights. In *A–F*, each symbol represents data from one mouse with 6 to 11 mice per group, horizontal bars denote means, and *P* values were determined by one-way ANOVA with Tukey's posttest. $*P < 0.05$; $**P < 0.01$.

neuromuscular junction remodeling pathways) and may reflect deactivation of catabolic/proatrophy signaling pathways that are otherwise activated in skeletal muscle during cancer, as well as simultaneous activation of anabolic/antiatrophy signaling pathways that are otherwise deactivated in skeletal muscle during cancer. Ursolic acid's effects on skeletal muscle mRNA expression also seem consistent with the way that we originally identified it, namely, by searching for small molecules whose global effects on mRNA expression in human cell lines are opposite to conserved changes in mRNA expression in skeletal muscle from two species (human and mouse) under two diverse atrophy conditions (prolonged fasting and spinal cord injury) (6). In that original screen, our bait represented the total transcriptional output of all catabolic/proatrophy signaling pathways that are induced and all anabolic/antiatrophy signaling pathways that are repressed under diverse atrophy conditions, and ursolic acid emerged as a molecule that could counteract that complex mixture of positive and negative transcriptional changes (6).

In human health and animal health, ursolic acid could be readily investigated as a nutritional approach for patients with cancer. In collaboration with industry, we recently developed, optimized, and commercialized ursolic acid as a dietary supplement for muscle health in dogs and cats (30), and we are nearing completion of similar translational work on ursolic acid for human nutrition. As a nutritional approach to cancer-induced skeletal muscle atrophy, ursolic acid could be a useful adjunct to other approaches that are currently used or in development, including tumor-directed therapies, physical therapy, conventional nutrition, and appetite stimulants. Ursolic acid could also be an important lead compound for pharmaceuticals for cancer-induced skeletal muscle atrophy, which currently lacks a muscle-directed pharmacologic therapy.

Limitations of the study include its exclusive use of mouse and cultured cell models, its exclusive use of male animals, the absence of additional functional readouts such as endurance exercise capacity, and the absence of investigations into whether ursolic acid may impact systemic inflammatory mediators of cachexia and/or generate more subtle changes in tumor cell biology. In future studies, it will be important to move beyond mouse and cultured cell models and investigate ursolic acid's effects in both females and males. It will also be important to perform deeper investigations of ursolic acid's effects on muscle function, systemic inflammatory mediators, and tumor cell biology.

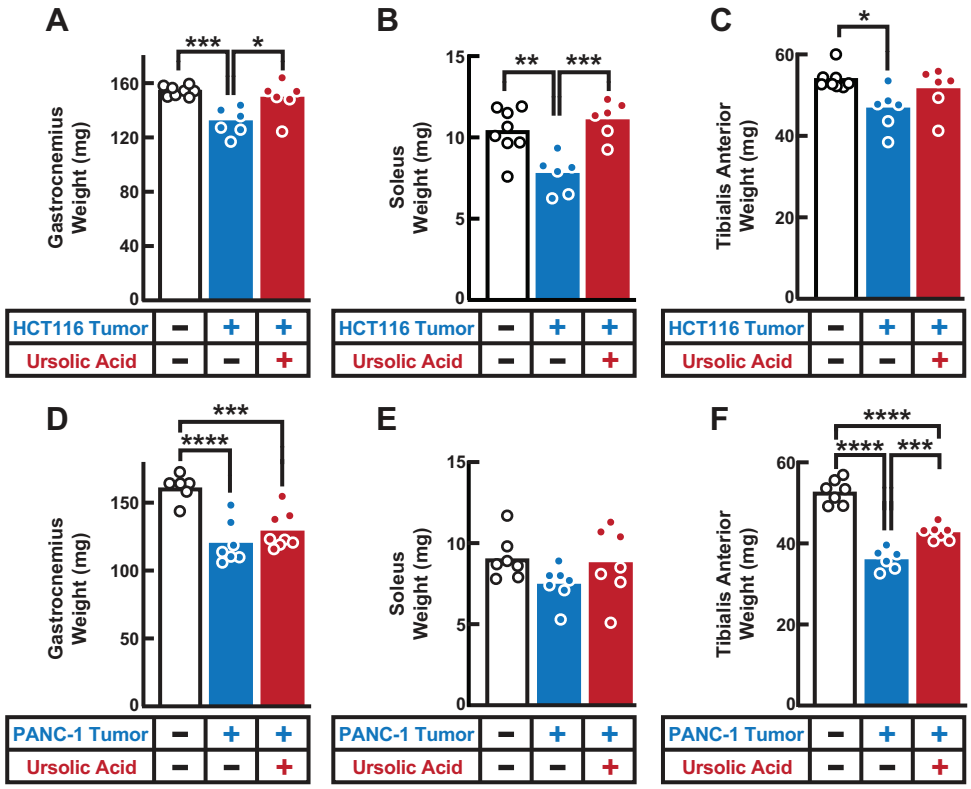

Figure 8. Ursolic acid reduces muscle wasting in mouse models that employ human colon and pancreatic cancers. *A–C*: eleven-week-old male *NOD.Cg-Prkdc^{scid} Il2rg^{tm1Wjl}/SzJ* (NSG) mice were administered bilateral flank injections of either saline ("Sham") or HCT116 human colorectal carcinoma cells ("HCT116"). On *day 9*, when HCT116 mice began to exhibit palpable tumors, half of HCT116 mice were provided ad libitum access to standard chow containing 0.27% ursolic acid ("HCT116 + Ursolic Acid"), and the remaining mice ("Sham" and "HCT116") continued to receive ad libitum access to standard chow lacking ursolic acid. On *day 22*, mice were euthanized for assessment of gastrocnemius (*A*), soleus (*B*), and tibialis anterior (*C*) weights. *D–F*: ten-week-old male NSG mice were administered intrapancreatic injections of saline ("Sham") or PANC-1 cells derived from a human exocrine pancreatic carcinoma ("PANC-1"). On *day 15*, when PANC-1 mice began to exhibit palpable tumors, half of PANC-1 mice were provided ad libitum access to standard chow containing 0.27% ursolic acid ("PANC-1 + Ursolic Acid"), and the remaining mice ("Sham" and "PANC-1") continued to receive ad libitum access to standard chow lacking ursolic acid. On *day 48*, mice were euthanized for assessment of gastrocnemius (*D*), soleus (*E*), and tibialis anterior (*F*) weights. In *A–F*, each symbol represents data from one mouse with 6 to 11 mice per group, horizontal bars denote means, and *P* values were determined by one-way ANOVA with Tukey's posttest. *$P < 0.05$; **$P < 0.01$; ***$P < 0.001$; ****$P < 0.0001$.

In conclusion, the current results provide robust evidence that dietary supplementation with ursolic acid can help to protect skeletal muscle mass in mouse models of cancer cachexia. These findings create an important foundation for nutritional studies in humans and companion animals, aimed at improving cancer management and outcomes through preservation of skeletal muscle structure and function.

DATA AVAILABILITY

Raw sequencing data are publicly available as of the date of publication at GEO: GSE325158.

SUPPLEMENTAL MATERIAL

Supplemental Figs. S1–S4 and Supplemental Table S1: https://doi.org/10.6084/m9.figshare.32129449.

ACKNOWLEDGMENTS

Graphical abstract created with a licensed version of BioRender.com.

GRANTS

This work was supported by funding from the US Department of Veterans Affairs Grant I01BX00976 (to C.M.A.), Florida Department of Health Bankhead-Coley Cancer Research Grant 21B05 (to A.R.J. and S.M.J.), and the US National Institutes of Health Grant R44CA277853 (to Emmyon, Inc., with S.M.E., C.M.A., A.R.J., S.M.J., and J.J.T. as multi-PIs). J.B.D. was supported by the NCI T32 training Grant T32CA257923 and the UF Health Cancer Institute, which is supported in part by state appropriations provided in Fla. Stat. §381.915 and the NCI Grant P30CA247796.

DISCLOSURES

C.M.A. is an inventor on granted patents for uses of ursolic acid to preserve muscle mass and function. Those patents are owned by the University of Iowa Research Foundation and the US Department of Veterans Affairs and are exclusively licensed to Emmyon, Inc. C.M.A., S.M.E., J.J.T., and A.R.J. are shareholders in Emmyon, Inc., where C.M.A., S.M.E., and J.J.T. are officers, and A.R.J. is a consultant and scientific advisory board member. Emmyon, Inc. shareholders participated in study design, data analyses and interpretation (C.M.A., S.M.E., J.J.T., and A.R.J.), and in data collection (A.R.J.). None of the other authors has any conflicts of interest, financial or otherwise, to disclose.

AUTHOR CONTRIBUTIONS

J.B.D., S.M.E., S.M.J., C.M.A., and A.R.J. conceived and designed research; J.B.D., M.E.C., M.M.S., C.S.C., A.C.D., J.J.T., S.M.J., and A.R.J. performed experiments; J.B.D., S.M.E., M.E.C., C.S.C., A.C.D., S.M.J., C.M.A., and A.R.J. analyzed data; J.B.D., S.M.E., S.M.J., C.M.A., and A.R.J. interpreted results of experiments; J.B.D., S.M.E., C.M.A., and A.R.J. prepared figures; J.B.D., S.M.E., S.M.J., C.M.A., and A.R.J. drafted manuscript; J.B.D., S.M.E., C.M.A., and A.R.J. edited and revised manuscript; J.B.D., S.M.E., M.E.C., M.M.S., C.S.C., A.C.D., J.J.T., S.M.J., C.M.A., and A.R.J. approved final version of manuscript.

REFERENCES

1. **Baracos VE**, **Martin L**, **Korc M**, **Guttridge DC**, **Fearon KCH.** Cancer-associated cachexia. *Nat Rev Dis Primers* 4: 17105, 2018. doi:10.1038/nrdp.2017.105.
2. **Martin L**, **Birdsell L**, **Macdonald N**, **Reiman T**, **Clandinin MT**, **McCargar LJ**, **Murphy R**, **Ghosh S**, **Sawyer MB**, **Baracos VE.** Cancer cachexia in the age of obesity: skeletal muscle depletion is a powerful prognostic factor, independent of body mass index. *J Clin Oncol* 31: 1539–1547, 2013. doi:10.1200/JCO.2012.45.2722.
3. **Kazemi-Bajestani SM**, **Mazurak VC**, **Baracos V.** Computed tomography-defined muscle and fat wasting are associated with cancer clinical outcomes. *Semin Cell Dev Biol* 54: 2–10, 2016. doi:10.1016/j.semcdb.2015.09.001.
4. **Koh K**, **Scott R**, **Cespedes Feliciano EM**, **Janowitz T**, **Goncalves MD**, **White EP**, **Laird BJA**, **Haase K**, **Jamal-Hanjani M.** Cancer-associated cachexia: bridging clinical findings with mechanistic insights in human studies. *Cancer Discov* 15: 1543–1568, 2025. doi:10.1158/2159-8290.CD-25-0293.
5. **Adams CM**, **Ebert SM**, **Dyle MC.** Use of mRNA expression signatures to discover small molecule inhibitors of skeletal muscle atrophy. *Curr Opin Clin Nutr Metab Care* 18: 263–268, 2015. doi:10.1097/MCO.0000000000000159.
6. **Kunkel SD**, **Suneja M**, **Ebert SM**, **Bongers KS**, **Fox DK**, **Malmberg SE**, **Alipour F**, **Shields RK**, **Adams CM.** mRNA expression signatures of human skeletal muscle atrophy identify a natural compound that increases muscle mass. *Cell Metab* 13: 627–638, 2011. doi:10.1016/j.cmet.2011.03.020.
7. **Frighetto RTS**, **Welendorf RM**, **Nigro EN**, **Frighetto N**, **Siani AC.** Isolation of ursolic acid from apple peels by high speed counter-current chromatography. *Food Chem* 106: 767–771, 2008. doi:10.1016/j.foodchem.2007.06.003.
8. **Kunkel SD**, **Elmore CJ**, **Bongers KS**, **Ebert SM**, **Fox DK**, **Dyle MC**, **Bullard SA**, **Adams CM.** Ursolic acid increases skeletal muscle and brown fat and decreases diet-induced obesity, glucose intolerance and fatty liver disease. *PLoS One* 7: e39332, 2012. doi:10.1371/journal.pone.0039332.
9. **Ebert SM**, **Dyle MC**, **Bullard SA**, **Dierdorff JM**, **Murry DJ**, **Fox DK**, **Bongers KS**, **Lira VA**, **Meyerholz DK**, **Talley JJ**, **Adams CM.** Identification and small molecule inhibition of an activating transcription factor 4 (ATF4)-dependent pathway to age-related skeletal muscle weakness and atrophy. *J Biol Chem* 290: 25497–25511, 2015. doi:10.1074/jbc.M115.681445.
10. **Yu R**, **Chen JA**, **Xu J**, **Cao J**, **Wang Y**, **Thomas SS**, **Hu Z.** Suppression of muscle wasting by the plant-derived compound ursolic acid in a model of chronic kidney disease. *J Cachexia Sarcopenia Muscle* 8: 327–341, 2017. doi:10.1002/jcsm.12162.
11. **Tao W**, **Ouyang Z**, **Liao Z**, **Li L**, **Zhang Y**, **Gao J**, **Ma L**, **Yu S.** Ursolic acid alleviates cancer cachexia and prevents muscle wasting via activating SIRT1. *Cancers (Basel)* 15: 2378, 2023. doi:10.3390/cancers15082378.
12. **Bigford GE**, **Darr AJ**, **Bracchi-Ricard VC**, **Gao H**, **Nash MS**, **Bethea JR.** Effects of ursolic acid on sub-lesional muscle pathology in a contusion model of spinal cord injury. *PLoS One* 13: e0203042, 2018. doi:10.1371/journal.pone.0203042.
13. **Ebert SM**, **Nicolas CS**, **Schreiber P**, **Lopez JG**, **Taylor AT**, **Judge AR**, **Judge SM**, **Rasmussen BB**, **Talley JJ**, **Rème CA**, **Adams CM.** Ursolic acid induces beneficial changes in skeletal muscle mRNA expression and increases exercise participation and performance in dogs with age-related muscle atrophy. *Animals (Basel)* 14: 186, 2024. doi:10.3390/ani14020186.
14. **Sivaram N**, **McLaughlin PA**, **Han HV**, **Petrenko O**, **Jiang YP**, **Ballou LM**, **Pham K**, **Liu C**, **van der Velden AW**, **Lin RZ.** Tumor-intrinsic PIK3CA represses tumor immunogenicity in a model of pancreatic cancer. *J Clin Invest* 129: 3264–3276, 2019. doi:10.1172/JCI123540.
15. **Callaway CS**, **Delitto AE**, **Patel R**, **Nosacka RL**, **D'Lugos AC**, **Delitto D**, **Deyhle MR**, **Trevino JG**, **Judge SM**, **Judge AR.** IL-8 released from human pancreatic cancer and tumor-associated stromal cells signals through a CXCR2-ERK1/2 axis to induce muscle atrophy. *Cancers (Basel)* 11: 1863, 2019. doi:10.3390/cancers11121863.
16. **Delitto D**, **Judge SM**, **Delitto AE**, **Nosacka RL**, **Rocha FG**, **DiVita BB**, **Gerber MH**, **George TJ Jr**, **Behrns KE**, **Hughes SJ**, **Wallet SM**, **Judge AR**, **Trevino JG.** Human pancreatic cancer xenografts recapitulate key aspects of cancer cachexia. *Oncotarget* 8: 1177–1189, 2017. doi:10.18632/oncotarget.13593.
17. **Neyroud D**, **D'Lugos AC**, **Trevino EJ**, **Callaway CS**, **Lamm J**, **Laitano O**, **Poole B**, **Deyhle MR**, **Brantley J**, **Le L**, **Judge AR**, **Judge SM.** Local inflammation precedes diaphragm wasting and fibrotic remodelling in a mouse model of pancreatic cancer. *J Cachexia Sarcopenia Muscle* 16: e13668, 2025. doi:10.1002/jcsm.13668.
18. **Huot JR**, **Novinger LJ**, **Pin F**, **Bonetto A.** HCT116 colorectal liver metastases exacerbate muscle wasting in a mouse model for the study of colorectal cancer cachexia. *Dis Model Mech* 13: dmm043166, 2020. doi:10.1242/dmm.043166.
19. **Bonetto A**, **Aydogdu T**, **Kunzevitzky N**, **Guttridge DC**, **Khuri S**, **Koniaris LG**, **Zimmers TA.** STAT3 activation in skeletal muscle links muscle wasting and the acute phase response in cancer cachexia. *PLoS One* 6: e22538, 2011. doi:10.1371/journal.pone.0022538.
20. **Reed SA**, **Sandesara PB**, **Senf SM**, **Judge AR.** Inhibition of FoxO transcriptional activity prevents muscle fiber atrophy during cachexia and induces hypertrophy. *FASEB J* 26: 987–1000, 2012. doi:10.1096/fj.11-189977.
21. **Wang C**, **Huo X**, **Gao L**, **Sun G**, **Li C.** Hepatoprotective effect of carboxymethyl pachyman in fluorouracil-treated CT26-bearing mice. *Molecules* 22: 756, 2017. doi:10.3390/molecules22050756.
22. **Neyroud D**, **Nosacka RL**, **Callaway CS**, **Trevino JG**, **Hu H**, **Judge SM**, **Judge AR.** FoxP1 is a transcriptional repressor associated with cancer cachexia that induces skeletal muscle wasting and weakness. *J Cachexia Sarcopenia Muscle* 12: 421–442, 2021. doi:10.1002/jcsm.12666.
23. **Moorwood C**, **Liu M**, **Tian Z**, **Barton ER.** Isometric and eccentric force generation assessment of skeletal muscles isolated from murine models of muscular dystrophies. *J Vis Exp*: e50036, 2013. doi:10.3791/50036.
24. **Ducharme JB**, **Carelock ME**, **Schonk MM**, **Al-Zaeed NM**, **Zhang W**, **Judge SM**, **Judge AR.** Identification of a senescence-associated transcriptional program in skeletal muscle of cachectic pancreatic-tumor-bearing mice. *Am J Physiol Cell Physiol* 328: C1125–C1134, 2025. doi:10.1152/ajpcell.00816.2024.
25. **Rupert JE**, **Narasimhan A**, **Jengelley DHA**, **Jiang Y**, **Liu J**, **Au E**, **Silverman LM**, **Sandusky G**, **Bonetto A**, **Cao S**, **Lu X**, **O'Connell TM**, **Liu Y**, **Koniaris LG**, **Zimmers TA.** Tumor-derived IL-6 and trans-signaling among tumor, fat, and muscle mediate pancreatic cancer cachexia. *J Exp Med* 218: e20190450, 2021. doi:10.1084/jem.20190450.
26. **Tomaz da Silva M**, **Roy A**, **Vuong AT**, **Joshi AS**, **Josphien C**, **Trivedi MV**, **Hindi SM**, **Narkar VA**, **Kumar A.** The TWEAK/Fn14 signaling mediates skeletal muscle wasting during cancer cachexia. *iScience* 28: 112714, 2025. doi:10.1016/j.isci.2025.112714.
27. **Sandri M**, **Sandri C**, **Gilbert A**, **Skurk C**, **Calabria E**, **Picard A**, **Walsh K**, **Schiaffino S**, **Lecker SH**, **Goldberg AL.** Foxo transcription factors induce the atrophy-related ubiquitin ligase atrogin-1 and cause skeletal muscle atrophy. *Cell* 117: 399–412, 2004. doi:10.1016/s0092-8674(04)00400-3.
28. **Stitt TN**, **Drujan D**, **Clarke BA**, **Panaro F**, **Timofeyva Y**, **Kline WO**, **Gonzalez M**, **Yancopoulos GD**, **Glass DJ.** The IGF-1/PI3K/Akt pathway prevents expression of muscle atrophy-induced ubiquitin ligases by inhibiting FOXO transcription factors. *Mol Cell* 14: 395–403, 2004. doi:10.1016/s1097-2765(04)00211-4.
29. **Chen L**, **Chen Y**, **Wang M**, **Lai L**, **Zheng L**, **Lu H.** Ursolic acid alleviates cancer cachexia by inhibiting STAT3 signaling pathways in C2C12 myotube and CT26 tumor-bearing mouse model. *Eur J Pharmacol* 969: 176429, 2024. doi:10.1016/j.ejphar.2024.176429.
30. **Virbac Corporation.** URSOLYX Soft Chews (Online). Virbac Group of Companies, 2026. https://us.virbac.com/products/Mobility/ursolyxTM-soft-chews [2026 Apr 27].